

ИИ
I-65

Inorganic Chemistry

including bioinorganic chemistry

June 3, 2013
Volume 52, Number 11
pubs.acs.org/IC

$\Delta O.D.$
0.04
0.00
-0.04
-0.08
-0.12
= 87.2 μs
400 500 600 700
Wavelength / nm

$\Delta O.D.$
0.01
0.00
-0.01
-0.02
-0.03
-0.04
 $\tau_T = 23.7 \mu s$
400 500 600 700
Wavelength / nm

1O_2
 T_1
 S_0
 $\Phi_\Delta \approx 52\%$
 3O_2

1O_2
 T_1
 S_0
 $\Phi_\Delta = 97\%$
 3O_2

Roadmap to Triplet Excited States



ACS Publications
MOST TRUSTED. MOST CITED. MOST READ.

www.acs.org

ON THE COVER: Two C[∞]N cyclometalated Ir(III) complexes containing a boron–dipyrromethane (Bodipy) chromophore were prepared, featuring different linkages between the Bodipy unit and the Ir(III) coordination center. The complex with a π -conjugated linker shows higher efficiency in singlet oxygen (¹O₂) production and triplet–triplet annihilation upconversion than the complex with a non- π -conjugated linker. See J. Sun, F. Zhong, X. Yi, and J. Zhao, p 6299.

Communications

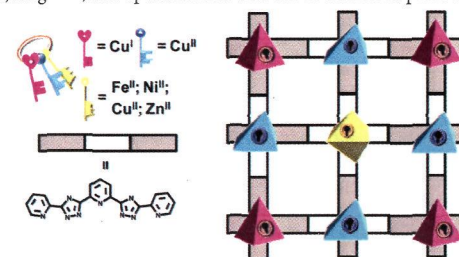
6233 

[dx.doi.org/10.1021/ic302808m](https://doi.org/10.1021/ic302808m)

Programmed Self-Assembly of Heterometallic [3 × 3] Grid [M^{II}Cu^I₄Cu^{II}]₄ (M = Fe, Ni, Cu, and Zn)

Xin Bao, Wei Liu, Ling-Ling Mao, Shang-Da Jiang, Jun-Liang Liu, Yan-Cong Chen, and Ming-Liang Tong*

A series of heterometallic [3 × 3] grids have been synthesized readily through a one-pot solvothermal reaction. Given metal ions carrying distinct electronic, magnetic, and optical information can be addressed precisely at specific locations in the array.



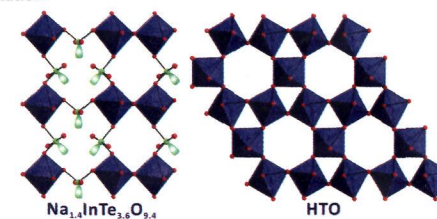
6236 

[dx.doi.org/10.1021/ic4009152](https://doi.org/10.1021/ic4009152)

Na_{1.4}InTe_{3.6}O_{9.4}: New Variant of a Hexagonal Tungsten Oxide (HTO)-Like Layered Framework Containing Both a Main-Group Cation, In³⁺, and a Lone-Pair Cation, Te⁴⁺

Dong Woo Lee and Kang Min Ok*

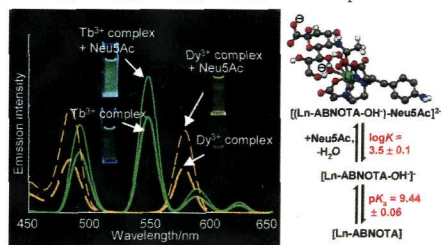
The first hexagonal tungsten oxide (HTO)-like layered framework containing both a main-group cation from the p block, In³⁺, and a lone-pair cation, Te⁴⁺, has been synthesized and characterized. The layered material changes to the three-dimensional framework in a dilute acidic solution.



New Molecular Motif for Recognizing Sialic Acid Using Emissive Lanthanide–Macrocyclic Polyazacarboxylate Complexes: Deprotonation of a Coordinated Water Molecule Controls Specific Binding

Kazuki Ouchi, Shingo Saito,* and Masami Shibukawa

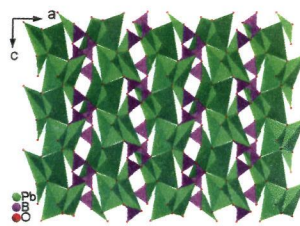
A new molecular motif—lanthanide–macrocyclic polyazacarboxylate hexadentate complexes, Ln^{3+} -ABNOTA—was found to specifically bind to sialic acid with strong emission enhancement and high affinity. The selectivity toward sialic acid over other monosaccharides was one of the highest among artificial receptors. Also, the novel binding mechanism was investigated in detail; binding selectivity is controlled by interactions between sialic acid and both the central metal and a hydroxyl group produced by deprotonation of a coordinated water molecule in the Ln^{3+} complex.



Facile Assembly of an Unusual Lead Borate with Different Cluster Building Units via a Hydrothermal Process

Han-Rui Tian, Wen-Hua Wang, Yan-E Gao, Ting-Ting Deng, Jia-Ying Wang, Yun-Long Feng, and Jian-Wen Cheng*

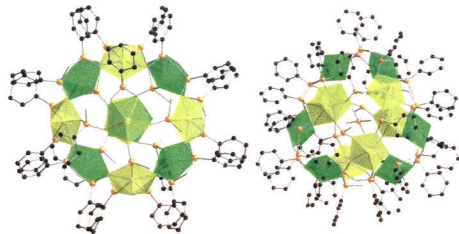
The first 5,9-connected lead borate, $\text{Pb}_6\text{B}_4\text{O}_{11}(\text{OH})_2$, built by different cluster building units of $\{\text{B}_4\}$ and $\{\text{Pb}_6\}$ has been obtained under mild hydrothermal conditions.



Hybrid Uranyl Arsonate Coordination Nanocages

Pius O. Adelani, Ginger E. Sigmon, and Peter C. Burns*

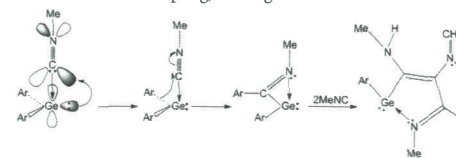
Nanosopic uranyl coordination cages have been prepared by a facile route involving self-assembly via temperature and solvent-driven, in situ ligand synthesis. The synthesis of hydrogen arsonate and pyroarsonate ligands in situ enhances flexibility, which is an important factor in producing these compounds.



Mechanisms of Reactions of Open-Shell, Heavier Group 14 Derivatives with Small Molecules: $n-\pi^*$ Back-Bonding in Isocyanide Complexes, C–H Activation under Ambient Conditions, CO Coupling, and Ancillary Molecular Interactions

Zachary D. Brown and Philip P. Power*

The complexation of isocyanides to germynes is stabilized by significant $n-\pi^*$ back-bonding. The buildup of the electron density at germanium leads to further reaction, leading to migratory insertion of isocyanide carbon into a germanium carbon bond, and the insertion of further isocyanides, leading to C–H activation. The reactivity pattern is paralleled by that of CO, which also leads to migratory insertion and CO coupling, leading to C–C bond activation.

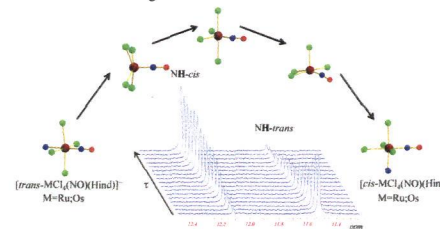


Articles

Mechanism Elucidation of the *cis*–*trans* Isomerization of an Azole Ruthenium–Nitrosyl Complex and Its Osmium Counterpart

Anatolie Gavriluta, Gabriel E. Büchel, Leon Freitag, Ghenadie Novitchi,* Jean Bernard Tommasino, Erwann Jeanneau, Paul-Steffen Kuhn, Leticia González,* Vladimir B. Arion,* and Dominique Luneau*

The *cis* and *trans* isomers of ruthenium and osmium nitrosyl complexes with general formulas $(n\text{Bu}_4\text{N})[\text{MCl}_4(\text{NO})(\text{Hind})]$ ($\text{M} = \text{Ru}$ or Os) have been synthesized and their crystal structures determined. NMR spectroscopy shows that the *cis* and *trans* complexes are stable in DMSO and $\text{C}_2\text{D}_2\text{Cl}_4$ solutions at room temperature, and *cis*/*trans* isomerization occurs at high temperatures (80–100 °C) and follows a reversible first order process with a dissociative mechanism as supported by electrochemical and theoretical calculations investigations.

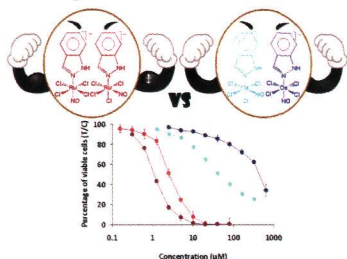


6273

dx.doi.org/10.1021/ic400555k

Striking Difference in Antiproliferative Activity of Ruthenium- and Osmium-Nitrosyl Complexes with Azole Heterocycles
Gabriel E. Büchel, Anatolie Gavriluta, Maria Novak, Samuel M. Meier, Michael A. Jakupec, Oleseza Cuzan, Constantin Turta, Jean-Bernard Tommasino, Erwann Jeanneau, Ghenadie Novitchi, Dominique Luneau,* and Vladimir B. Arion*

The effects of metal (Ru vs Os), cis/trans isomerism, and azole heterocycle identity on in vitro anticancer potency of $[\text{MCl}_4(\text{NO})(\text{Hazole})]^-$ (M = Ru, Os) complexes were elucidated. In contrast to most pairs of isostructural ruthenium and osmium complexes known, ruthenium complexes, yielding IC_{50} values in the low micromolar concentration range, are considerably more cytotoxic than osmium analogues.



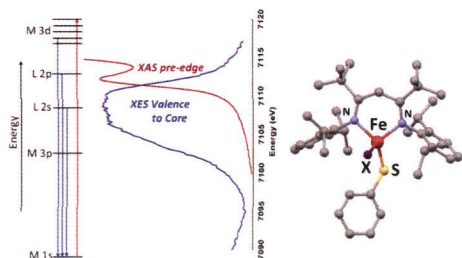
6286

dx.doi.org/10.1021/ic3021723

Sensitivity of X-ray Core Spectroscopy to Changes in Metal Ligation: A Systematic Study of Low-Coordinate, High-Spin Ferrous Complexes

P. Chandrasekaran, Karen P. Chiang, Dennis Nordlund, Uwe Bergmann, Patrick L. Holland,* and Serena DeBeer*

X-ray absorption (XAS) and X-ray emission (XES) spectra of iron complexes $[\text{L}^{\text{tbu}}\text{Fe}(\text{SPh})(\text{X})]$ (X = CN^tBu, 1-methylimidazole, DMF) were analyzed in order to understand the sensitivity of these techniques to variations in the ligation sphere on iron. The experimental data were correlated to calculations and extended to a hypothetical test set of molecules, which allowed systematic examination of the contributions of metal oxidation state, ligand identity, ionization potential, and protonation state.



8A

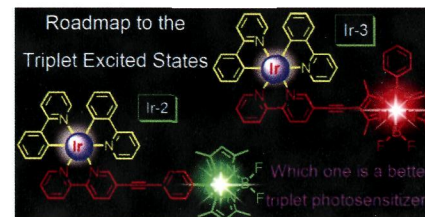
Inorganic Chemistry, Volume 52, Issue 11

6299

dx.doi.org/10.1021/ic302210b

Efficient Enhancement of the Visible-Light Absorption of Cyclometalated Ir(III) Complexes Triplet Photosensitizers with Bodipy and Applications in Photooxidation and Triplet–Triplet Annihilation Upconversion
Jifu Sun, Fangfang Zhong, Xiuyu Yi, and Jianzhang Zhao*

Molecular designing strategies to enhance the effective visible-light absorbing of cyclometalated Ir(III) complexes by attaching Bodipy chromophores to the coordination center were reported. In one complex the two units were isolated from each other (Ir-2), and in another complex (Ir-3) π conjugation between the π core of Bodipy and the coordination center was established. Application of the complexes as triplet photosensitizers in singlet oxygen ($^1\text{O}_2$)-mediated photooxidation and triplet–triplet annihilation upconversion demonstrated that visible-light harvesting in Ir-3 is more efficient to produce triplet excited states.



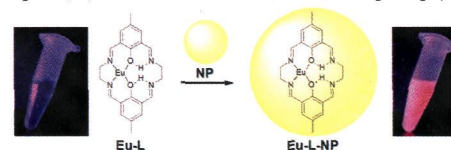
6311

dx.doi.org/10.1021/ic3022722

Turning on Lanthanide Luminescence via Nanoencapsulation

Boris Makhinson, Alexandra K. Duncan, Ashley R. Elam, Ana de Bettencourt-Dias, Colin D. Medley, Joshua E. Smith,* and Eric J. Werner*

Encapsulation of a macrocyclic europium(III) complex by discrete, monodisperse SiO_2 nanoparticles and the resultant dramatic effect on metal-derived luminescence are discussed. The free metal complex is readily synthesized and exhibits primarily weak ligand-derived emission at room temperature, displaying significant europium-centered luminescence only when cooled to 77 K. Upon encapsulation by the nanoparticles, however, metal luminescence is visibly “turned on” at room temperature, yielding strong europium(III) emission rationalized via a detailed photophysical study.



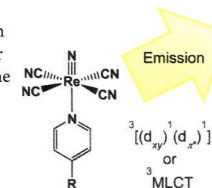
6319

dx.doi.org/10.1021/ic302463v

Excited-State Characteristics of Tetracyanonitridorhenium(V) and -technetium(V) Complexes with N-Heteroaromatic Ligands

Hayato Ikeda, Akitaka Ito, Eri Sakuda, Noboru Kitamura, Tsutomu Takayama, Tsutomu Sekine, Atsushi Shinohara, and Takashi Yoshimura*

The tetracyanonitridorhenium(V) and -technetium(V) complexes with N-heteroaromatic ligands have been synthesized, and their spectroscopic and photophysical properties have been characterized. The rhenium complexes exhibited two types of excited states ($^3[(d_{xy})^1(d_{xz})^1]$ or $^3\text{MLCT}$) by a change in the π^* level of the N-heteroaromatic ligand. On the other hand, all of the technetium complexes possessed $^3[(d_{xy})^1(d_{xz})^1]$ excited states.



9A

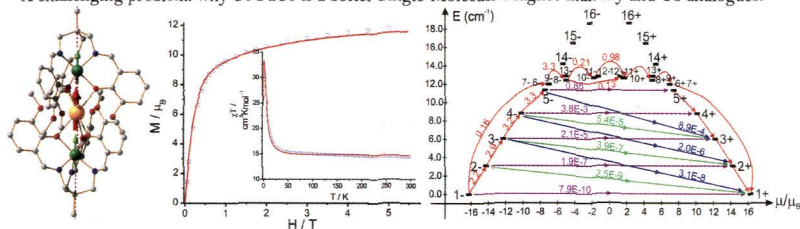
Inorganic Chemistry, Volume 52, Issue 11

Interplay of Strongly Anisotropic Metal Ions in Magnetic Blocking of Complexes

Liviu Ungur, Maarten Thewissen, Jean-Pierre Costes, Wolfgang Wernsdorfer, and Liviu F. Chibotaru*

Ab initio based analysis shows that a multilevel blocking barrier obtained for Co–Gd–Co is more efficient compared to blocking barriers of isostructural Co–Dy–Co and Co–Tb–Co involving fewer exchange states.

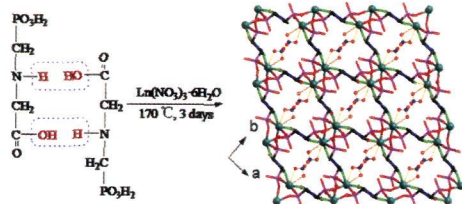
A challenging problem: why CoGdCo is a better Single-Molecule Magnet than Dy and Tb analogues?



Photoluminescent 3D Lanthanide–Organic Frameworks Based on 2,5-Dioxo-1,4-piperazinylbis(methylphosphonic) Acid Formed via In Situ Cyclodehydration of Glyphosates

Yunshan Zhou,* Yan Guo, Sheng Xu, Lijuan Zhang,* Waqar Ahmad, and Zonghai Shi

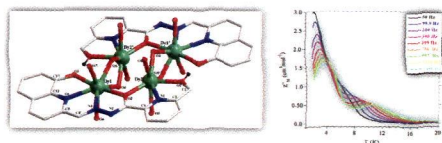
The hydrothermal reaction between lanthanide nitrates and glyphosate resulted in cyclodehydration of glyphosates and concomitant formation of three new 3D photoluminescent lanthanide–organic frameworks, Ln(NO₃)(H₂L) [Ln = Eu (1), Tb (2), Gd (3); H₂L = 2,5-dioxo-1,4-piperazinylbis(methylphosphonic) acid].



Rhombus-Shaped Tetranuclear [Ln₄] Complexes [Ln = Dy(III) and Ho(III)]: Synthesis, Structure, and SMM Behavior

Vadapalli Chandrasekhar,* Sakiat Hossain, Sourav Das, Sourav Biswas, and Jean-Pascal Sutter*

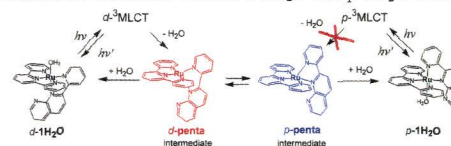
The reaction of a new hexadentate Schiff base hydrazide ligand (LH₃) with rare earth(III) chloride salts afforded two planar tetranuclear rhombus-shaped neutral complexes: [{(LH₂Dy₄)(μ₂-O)₄}(H₂O)₈·2CH₃OH·8H₂O (1) and [{(LH₂Ho₄)(μ₂-O)₄}(H₂O)₈·6CH₃OH·4H₂O (2). Complex 1 is an SMM and shows two relaxation processes that lead to two energy barriers (16.8 and 54.2 K) and time constants (τ₀ = 1.4 × 10⁻⁶ s, τ₁ = 7.2 × 10⁻⁷ s).



Mechanisms of Photoisomerization and Water-Oxidation Catalysis of Mononuclear Ruthenium(II) Monoaquo Complexes

Masanari Hirahara, Mehmed Z. Ertem, Manabu Komi, Hirotsato Yamazaki, Christopher J. Cramer, and Masayuki Yagi*

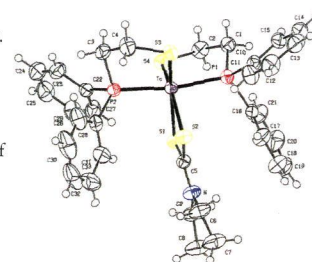
The mechanism of the photoisomerization of *distal*-[Ru(tpy)(pynp)OH₂]²⁺ (*d*-1H₂O) to *proximal* isomer (*p*-1H₂O) was investigated using a transient absorption spectroscopic technique and quantum chemical calculations. Proton-coupled electron transfer reactions (PCET) are different between *d*- and *p*-1H₂O isomers. Catalytic activity of *d*-1H₂O for water oxidation is higher than that for *p*-1H₂O. Quantum chemical calculations provide redox potentials and pK_a values indicating PCET processes and further explain mechanistic differences between *d*-1H₂O and *p*-1H₂O with respect to water oxidation.



Synthesis and Characterization of [M^{III}(PS)₂(L)] Mixed-Ligand Compounds (M = Re, ⁹⁹Tc; PS = Phosphinothiolate; L = Dithiocarbamate) as Potential Models for the Development of New Agents for SPECT Imaging and Radiotherapy

N. Salvarese,* N. Morellato, A. Venzo, F. Refosco, A. Dolmella, and C. Bolzati*

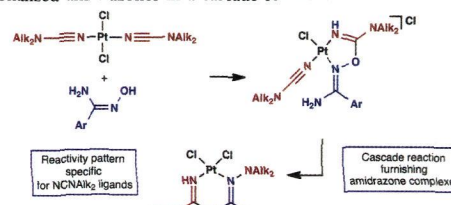
This article reports a reactivity study of bis(arylalkyl)- and trialkylphosphinothiol (PSH) and dithiocarbamate (L) ligands toward M^{III}/V/VII (M = ⁹⁹Tc/Re) precursors. A new series of neutral, six-coordinated mixed-ligand compounds [M^{III}(PS)₂(L)] (M = Re; ⁹⁹Tc), where PS is bis(arylalkyl)- or trialkylphosphinothiolate and L is dithiocarbamate, are reported. The opportunity of easily preparing these [M^{III}(PS)₂(L)] complexes, in mild reactions conditions and in high yield, starting from the corresponding permethylate anions, lays the first stone to the preparation of a new series of M^{III}-based (M = ^{99m}Tc/¹⁸⁸Re) compounds useful in theragnostic applications.



Amidrazone Complexes from a Cascade Platinum(II)-Mediated Reaction between Amidoximes and Dialkylcyanamides

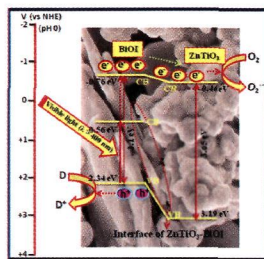
Dmitrii S. Bolotin, Nadezhda A. Bokach,* Andreii S. Kritchenkov, Matti Haukka, and Vadim Yu. Kukushkin*

Products of Pt^{II}-mediated coupling of dialkylcyanamides and amidoximes, viz. the chelated iminoacylated amidoximes, easily convert to metal-bound functionalized amidrazones in a cascade reaction.



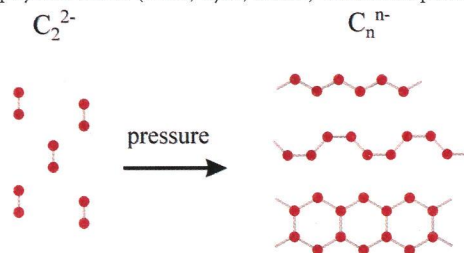
6390 [dx.doi.org/10.1021/ic400159m](https://doi.org/10.1021/ic400159m)
Fabrication of Novel p-BiOI/n-ZnTiO₃ Heterojunction for Degradation of Rhodamine 6G under Visible Light Irradiation
 K. Hemalata Reddy, Satyabadi Martha, and K.M. Parida*

The broad visible light absorption, efficient charge carrier excitation, and their separation in the p-BiOI/n-ZnTiO₃ heterojunction enhance the photocatalytic activity to a great extent.



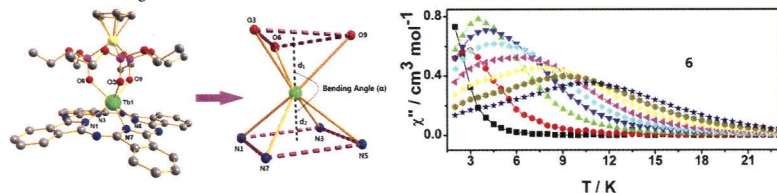
6402 [dx.doi.org/10.1021/ic4002219](https://doi.org/10.1021/ic4002219)
Lithium and Calcium Carbides with Polymeric Carbon Structures
 Daryn Benson, Yanling Li, Wei Luo, Rajeev Ahuja, Gunnar Svensson, and Ulrich Häussermann*

We studied the binary carbide systems Li₂C₂ and CaC₂ at high pressure using evolutionary and ab initio random structure search methodology for crystal structure prediction. At ambient pressure Li₂C₂ and CaC₂ represent salt-like acetylides consisting of C₂²⁻ dumbbell anions. The systems develop into semimetals (P3m1-Li₂C₂) and metals (Cmcm-Li₂C₂, Cmcm-CaC₂, and Immm-CaC₂) with polymeric anions (chains, layers, strands) at moderate pressures (below 20 GPa).



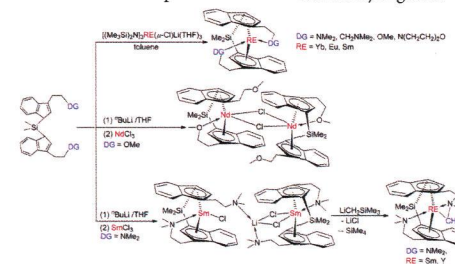
6407 [dx.doi.org/10.1021/ic400245n](https://doi.org/10.1021/ic400245n)
Syntheses, Structures, and Magnetic Properties of seven-coordinate Lanthanide Porphyrinate or Phthalocyaninate Complexes with Kläui's Tripodal Ligand
 Feng Gao, Min-Xia Yao, Yu-Yang Li, Yi-Zhi Li, You Song,* and Jing-Lin Zuo*

Eight new seven-coordinate mononuclear lanthanide(III) complexes of the general formula [(TPP)Ln(L_{OR})₂]-0.25H₂O and [(Pc)Ln(L_{OR})₂] (Ln³⁺ = Dy³⁺, Tb³⁺, Ho³⁺, and Gd³⁺; TPP = 5,10,15,20-tetraphenylporphyrinate; Pc = phthalocyaninate; L_{OR}⁻ = [(η⁵-C₅H₅)Co(P(=O)(OEt)₂)₃]⁻) have been synthesized. All of the compounds exhibit a similar double-decker sandwich structure. The Dy and Tb complexes show the field-induced slow relaxation of magnetization, and they are rare seven-coordinate single-lanthanide-based SMMs. The coordination geometry around the Ln³⁺ ions in the porphyrin and the phthalocyanine systems, such as metal-to-plane distances, plane center distances, and bending angles, is slightly different, leading to their different magnetic behaviors.



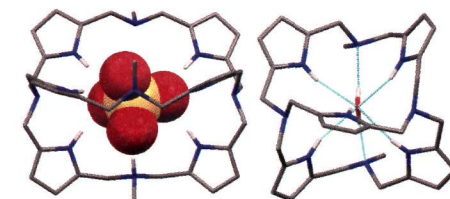
6417 [dx.doi.org/10.1021/ic4003109](https://doi.org/10.1021/ic4003109)
Controlled Synthesis of Racemic Indenyl Rare-Earth Metal Complexes via the Cooperation between the Intramolecular Coordination of Donor Atoms and a Bridge

Shuangliu Zhou,* Zhangshuan Wu, Lingmin Zhou, Shaowu Wang,* Lijun Zhang, Xiancui Zhu, Yun Wei, Jinhua Zhai, and Jie Wu
 A methodology featuring the cooperative interaction between a Me₂Si bridge and coordinative heteroatoms was developed, enabling the controlled syntheses of racemic indenyl rare-earth metal complexes. This methodology provides facile access to racemic divalent and trivalent rare-earth metal complexes with different indenyl ligands.



6427 [dx.doi.org/10.1021/ic400319b](https://doi.org/10.1021/ic400319b)
Synthesis of Novel Polyazacryptands for Recognition of Tetrahedral Oxanions and Their X-ray Structures
 Debasish Jana, Ganesan Mani,* and Carola Schulzke

A new class of pyrrole-based pentaaza- and tetraazacryptand derivatives were synthesized and structurally characterized. Anion binding properties of these macrobicycles were studied by ¹H and ¹⁹F NMR methods. The structures of the inclusion complexes of chloride, sulfate, phosphate, and arsenate ions were confirmed by X-ray diffraction method, showing the anion induced conformational changes to the macrobicyclic and the existence of strong hydrogen bonding. The competition crystallization experiment using the pentaazacryptand yielded its phosphate anion complex as a sole product in the presence of other anions in aqueous-organic medium.

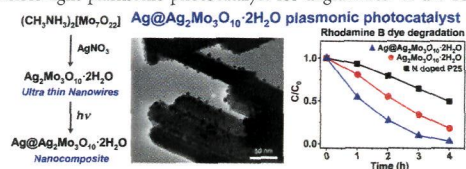


Cl⁻, SO₄²⁻, H_xPO₄^{(3-x)-}, H_xAsO₄^{(3-x)-} cryptates

Novel Soft-Chemistry Route of $\text{Ag}_2\text{Mo}_3\text{O}_{10}\cdot 2\text{H}_2\text{O}$ Nanowires and in Situ Photogeneration of a $\text{Ag}@\text{Ag}_2\text{Mo}_3\text{O}_{10}\cdot 2\text{H}_2\text{O}$ Plasmonic Heterostructure

Khadija Hakouk, Philippe Deniard, Luc Lajaunie, Catherine Guillot-Deudon, Sylvie Harel, Zeyan Wang, Baibiao Huang, Hyun-Joo Koo, Myung-Hwan Whangbo, Stéphane Jobic, and Rémi Dessapt*

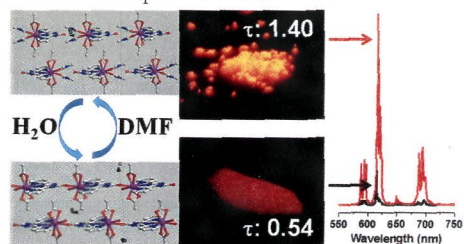
Very thin $\text{Ag}_2\text{Mo}_3\text{O}_{10}\cdot 2\text{H}_2\text{O}$ nanowires (NWs) have been successfully prepared via a new soft-chemistry route. Under UV irradiation, Ag^0 nanoparticles are easily in situ generated, and the resulting $\text{Ag}@\text{Ag}_2\text{Mo}_3\text{O}_{10}\cdot 2\text{H}_2\text{O}$ heterostructure has been characterized by TEM, Auger, XPS, UV-vis, and EELS analyses revealing that both Ag^+ and Mo^{6+} ions are photoreduced. A mechanism is proposed which involves oxidation of the crystallized water molecules. The $\text{Ag}@\text{Ag}_2\text{Mo}_3\text{O}_{10}\cdot 2\text{H}_2\text{O}$ nanocomposite is an efficient visible-light plasmonic photocatalyst for degradation of the RhB dye.



Solvent-Mediated Crystal-to-Crystal Interconversion between Discrete Lanthanide Complexes and One-Dimensional Coordination Polymers and Selective Sensing for Small Molecules

Jin-Ji Wu, Yu-Xin Ye, Ying-Yu Qiu, Zheng-Ping Qiao, Man-Li Cao,* and Bao-Hui Ye*

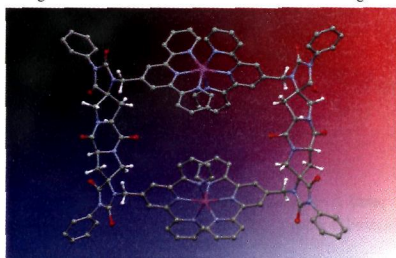
Reversible crystal-to-crystal transformation between discrete lanthanide complexes and 1D coordination polymers were realized by immersing the crystals in the corresponding solvent or by exposing them to solvent vapor. Complex 1 shows a highly selective luminescence enhancement in response to DMF.



Architectural Spirologomers Designed for Binuclear Metal Complex Templating

Shivaiah Vaddypally, Chongsong Xu, Senzhi Zhao, Yanfeng Fan, Christian E. Schafmeister,* and Michael J. Zdilla*

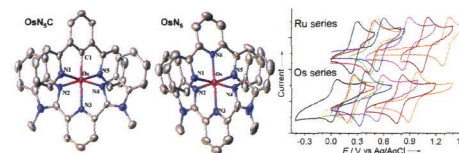
Ligand design has been a fruitful subfield of inorganic chemistry, but ligand synthesis is expensive and time consuming. Linkage of bis-amino acids to form spirologomers provides versatile designable ladder oligomers with programmable shapes and functional group displays for binding of transition metal ions in desired configurations.



Monometallic Osmium(II) Complexes with Bis(*N*-methylbenzimidazolyl)benzene or -pyridine: A Comparison Study with Ruthenium(II) Analogues

Jiang-Yang Shao and Yu-Wu Zhong*

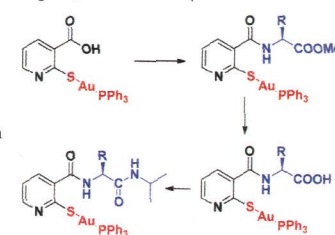
Seven bis-tridentate osmium complexes with Mebib or Mebip (Mebib is the 2-deprotonated form of 1,3-bis(*N*-methylbenzimidazolyl)benzene and Mebip is bis(*N*-methylbenzimidazolyl)pyridine) have been prepared. They have either the $[\text{Os}(\text{NCN})(\text{NNN})]$ - or $[\text{Os}(\text{NNN})(\text{NNN})]$ -type coordination mode. The Os(II/III) redox potentials of these complexes range from +0.04 to +0.94 V vs Ag/AgCl , which are 200–300 mV less positive relative to the Ru(II/III) potentials of their ruthenium structural analogues.



Synthesis of New Gold(I) Thiolates Containing Amino Acid Moieties with Potential Biological Interest

Alejandro Gutiérrez, Javier Bernal, M. Dolores Villacampa, Carlos Cativiela, Antonio Laguna, and M. Concepción Gimeno*

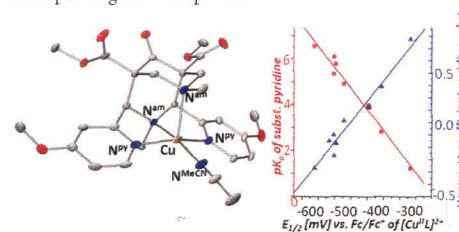
The reaction of the gold(I) complex $[\text{Au}(\text{SpyCOOH})(\text{PPh}_3)]$, which contains nicotinic acid thiolate, with several amino acid esters produces the gold(I) derivatives with the new thiolate containing amino acid ester ligands $[\text{Au}\{\text{SpyCONHCH}(\text{R})\text{COOMe}\}(\text{PPh}_3)]$. The reaction of these amino acid ester derivatives with LiOH in methanol and acidification with KHSO_4 afford the corresponding acids. These amino acid compounds can be further coupled with other amines, such as, for example, isopropylamine, to give the corresponding amide derivatives.




Tuning of the Properties of Transition-Metal Bispidine Complexes by Variation of the Basicity of the Aromatic Donor Groups

Peter Comba,* Michael Morgen, and Hubert Wadepohl

The redox potentials of Cu^{II} complexes with tetradentate bispidine ligands can be varied by substitution of the pyridine ring. Correlation of these redox potentials with either the $\text{p}K_a$ values of the pyridine groups or the Hammett parameters (or computed parameters from a DFT-based energy decomposition analysis) allows for an accurate prediction of the thermodynamic stability of the corresponding Cu^{II} complexes.

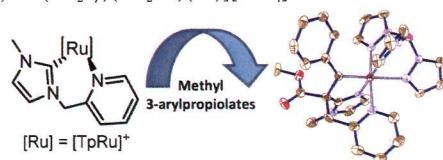


6502  dx.doi.org/10.1021/ic400433z

Functionalized N-Heterocyclic Carbene Nonspectator Ligands upon Internal Alkyne Activation Reactions

Francys E. Fernández, María del Carmen Puerta,* and Pedro Valerga*

When studying the activation of 3-arylpropiolates by [TpRu(picolyl-R¹)Cl]/NaBAR^F₄ (picolyl-M¹T = 3-methyl-1-(2-picolyl)imidazol-2-ylidene (1); picolyl-M²BI = 3-methyl-1-(2-picolyl)benzoimidazol-2-ylidene (2)) a migratory insertion of the NHC into a ruthenium-carbon bond and an unprecedented C-N bond activation of the chelating picolyl-NHC ligand take place to give the new ruthenium metallacycles [TpRu(κ^3 -C,N,N'-C(Ph)-C(CH₂Py)(CO₂Me)^(M¹))] [BAR^F₄] 3a and 4a and [TpRu(κ^3 -C,N,N'-C(4-CF₃Ph)-C(CH₂Py)(CO₂Me)^(M¹))] [BAR^F₄] 3b and 4b.

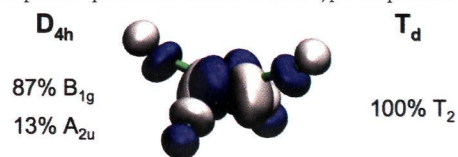


6510  dx.doi.org/10.1021/ic4004774

Pseudo-symmetry Analysis of the d-block Molecular Orbitals in Four-Coordinate Complexes

Andrés Falceto, David Casanova, Pere Alemany, and Santiago Alvarez*

How much of its symmetry does a molecular orbital preserve when a molecule is distorted or experiences asymmetric chemical substitution? Can we correlate its symmetry changes with the absorption intensity in the visible spectrum? Pseudo-symmetry concepts and tools are applied to provide quantitative answers to these types of questions.

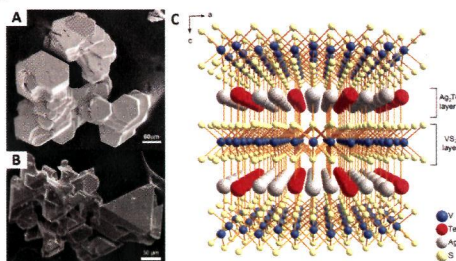


6520  dx.doi.org/10.1021/ic400483d

Lattice-Matched Transition Metal Disulfide Intergrowths: The Metallic Conductors Ag₂Te(MS₂)₃ (M = V, Nb)

Sandy L. Nguyen, Christos D. Malliakas, Melanie C. Francisco, and Mercouri G. Kanatzidis*

The stabilization of the intergrowth metallic compounds (Ag₂Te)(MS₂) adds a new type of intercalated motif to the class of transition metal dichalcogenides.

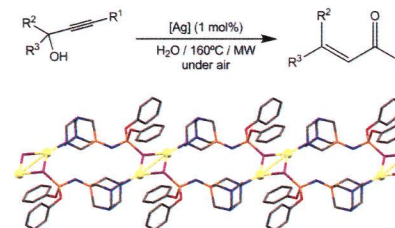


6533  dx.doi.org/10.1021/ic400511d

New Ag(I)-Iminophosphorane Coordination Polymers as Efficient Catalysts Precursors for the MW-Assisted Meyer-Schuster Rearrangement of Propargylic Alcohols in Water

Joaquín García-Alvarez,* Josefina Díez, Cristian Vidal, and Cristian Vicent

A new protocol for the selective Meyer-Schuster rearrangement of propargylic alcohols in water and under air has been developed using catalytic amounts of the new one-dimensional coordination polymers ([Ag{ μ^2 -N,S-(PTA)=NP(=S)(OR)₂}]_x[SbF₆]_x and [Ag{ μ^2 -O,S-(DAPTA)=NP(=S)(OR)₂}]_x[SbF₆]_x). Remarkably, the catalytic system can be reused in ten consecutive runs.

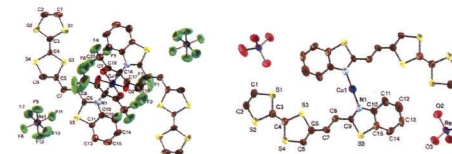


6543  dx.doi.org/10.1021/ic4005246

Cu^{II} and Cu^I Coordination Complexes Involving Two Tetrathiafulvalene-1,3-benzothiazole Hybrid Ligands and Their Radical Cation Salts

Sayo Yokota, Keiji Tsujimoto, Sadayoshi Hayashi, Fabrice Pointillart, Lahcène Ouahab, and Hideki Fujiwara*

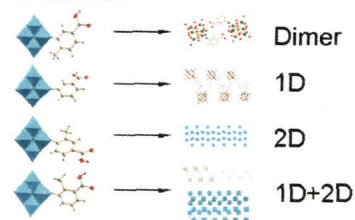
Preparations, crystal structure analyses, and magnetic property investigations on a new Cu^{II}(hfac)₂ complex coordinated with two TTF-CH=CH-BTA ligands, where hfac is hexafluoroacetylacetonate, TTF is tetrathiafulvalene, and BTA is 1,3-benzothiazole, are reported together with those of its dicationic AsF₆⁻ salt, [Cu(hfac)₂(TTF-CH=CH-BTA)₂](AsF₆)₂, in which each TTF part is in a radical cation state. Furthermore, crystal structure analysis and magnetic/conducting properties of a radical cation ReO₄⁻ salt of the Cu^I complex with two TTF-CH=CH-BTA ligands, [Cu(TTF-CH=CH-BTA)₂](ReO₄)₂, are also described.



Organoimido-Derivatized Hexamolybdates with a Remote Carboxyl Group: Syntheses and Structural Characterizations

Guohui Sima, Qiang Li, Yi Zhu, Chunlin Lv, Rao Naumaan Nasim Khan, Jian Hao, Jin Zhang,* and Yongge Wei*

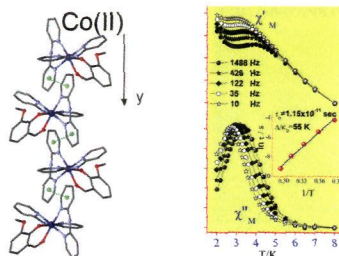
Four novel organoimido derivatives of hexamolybdate containing a remote carboxyl group have been synthesized by the reaction of octamolybdate and the corresponding hydrochlorides of the organic ligands: $[\text{Bu}_4\text{N}]_2[\text{Mo}_6\text{O}_{18}(\text{N}-\text{C}_6\text{H}_4-3-\text{COOH})]$ (1), $[\text{Bu}_4\text{N}]_2[\text{Mo}_6\text{O}_{18}(\text{N}-\text{C}_6\text{H}_4-2-\text{CH}_3-4-\text{COOH})]$ (2), $[\text{Bu}_4\text{N}]_2[\text{Mo}_6\text{O}_{18}(\text{N}-\text{C}_6\text{H}_4-2-\text{CH}_3-5-\text{COOH})]$ (3), and $[\text{Bu}_4\text{N}]_2[\text{Mo}_6\text{O}_{18}(\text{N}-\text{C}_6\text{H}_4-2-\text{CH}_3-3-\text{COOH})]$ (4). Hydrogen bonding interactions play an important role in the assemblies. The similar organic moieties in the organoimido products result in different behaviors of the supramolecular assemblies. The dimer, 1D, 2D, and 1D plus 2D structures are formed.



New Type of Single Chain Magnet: Pseudo-One-Dimensional Chain of High-Spin Co(II) Exhibiting Ferromagnetic Intrainchain Interactions

V. Tangoulis,* M. Lalia-Kantouri,* M. Gdaniec, Ch. Papadopoulos, V. Miletic, and A. Czapik

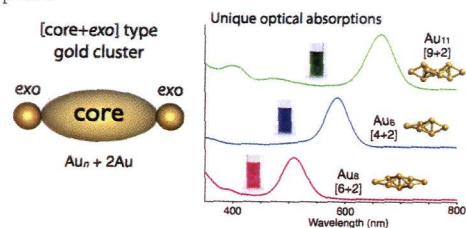
Two high-spin Co(II) complexes have been synthesized through the reactions of Co(II) salts with dipyrindylamine (dpamH) and 5-nitro-salicylaldehyde or 3-methoxy-salicylaldehyde: $[\text{Co}(\text{dpamH})_2(5-\text{NO}_2\text{-salo})\text{NO}_3]$ (1) and $[\text{Co}(\text{dpamH})_2(3-\text{OCH}_3\text{-salo})\text{NO}_3 \cdot 1.3 \text{ EtOH} \cdot 0.4\text{H}_2\text{O}]$ (2). In the first case the magnetic studies showed that the Co(II) ions are magnetically isolated while in the second compound a quite surprising SCM behavior is revealed due to pseudo-1D arrangement of the cations through $\pi-\pi$ stacking interactions between pyridine rings of one of the dpamH ligands.



Electronic Properties of [Core+exo]-type Gold Clusters: Factors Affecting the Unique Optical Transitions

Yukatsu Shichibu and Katsuaki Konishi*

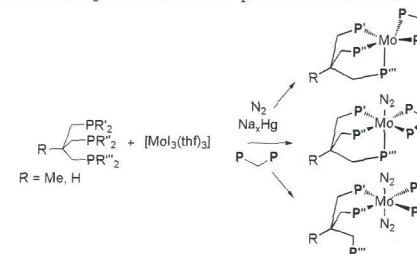
Optical properties of [core+exo]-type gold clusters, which show an unusual isolated visible absorption, were studied from experimental/theoretical aspects. Through studies on three clusters of different nuclearity, we have shown the absorption properties are dependent on the cluster geometry rather than the nuclearity. Theoretical results indicated that, for all the clusters, the exo gold atoms are critically involved in the generation of the HOMO and LUMO bands responsible for the appearance of the visible absorptions.



Bonding and Activation of N₂ in Mo(0) Complexes Supported by Hybrid Tripod Ligands with Mixed Dialkylphosphine/Diarylphosphine Donor Groups: Interplay of Steric and Electronic Factors

Ludger Sönksen, Christian Gradert, Jan Krahmer, Christian Näther, and Felix Tuczek*

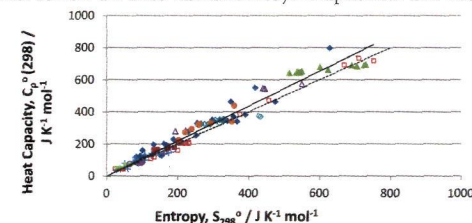
Molybdenum dinitrogen complexes are presented which are supported by novel hybrid tripod ligands of the type Me-C(CH₂PPh₂)₂(CH₂PⁱPr₂) (trpd-1) and H-C(CH₂PPh₂)(CH₂PⁱPr₂)₂ (trpd-2) having mixed dialkylphosphine/diarylphosphine donor groups. Reaction of the ligand trpd-1 with $[\text{MoI}_2(\text{thf})_3]$ followed by sodium amalgam reduction in the presence of the dpmm gives the dinitrogen complex $[\text{Mo}(\text{N}_2)(\text{trpd-1})(\text{dpmm})]$ where trpd-1 is coordinated in a κ^3 fashion. The complex exhibits a moderate activation of N₂ which enables its protonation under retention of the pentaphosphine ligation.



Ambient Heat Capacities and Entropies of Ionic Solids: A Unique View Using the Debye Equation

Leslie Glasser*

Ambient heat capacities and entropies of larger ionic solids, such as minerals, are similar in value. This unexpected relation is explained in terms of the Debye equation. The Debye temperature is easily calculated from the ratio C_p/S_p , showing that ionic solids whose ambient data points lie near the fitted line have Debye temperatures near 600 K.



Tetranuclear [MDy]₂ Compounds and Their Dinuclear [MDy] (M = Zn/Cu) Building Units: Their Assembly, Structures, and Magnetic Properties

Peng Zhang, Li Zhang, Shuang-Yan Lin, and Jinkui Tang*

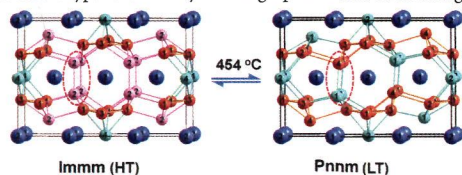
The assembly of [MDy]₂ aggregates containing two 3d-4f [MDy] (M = Zn or Cu) building blocks presents a promising strategy for constructing efficient heterometallic SMMs.



6603  dx.doi.org/10.1021/ic400626x

Disorder–Order Structural Transformation in Electron-Poor $Sr_3Au_8Sn_3$ Driven by Chemical Bonding Optimization
Qisheng Lin, Jordan Vetter, and John D. Corbett*

Structural transformation from the high-temperature form of La_3Al_{11} -type $Sr_3Au_8Sn_3$ (*Immm*) to its low-temperature form with $Ca_3Au_8Ge_3$ -type (*Pnmm*) structure type is driven by bonding optimization overcoming the entropy decrease.

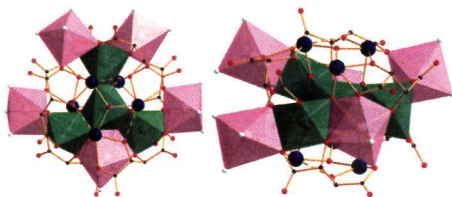



6610  dx.doi.org/10.1021/ic4006345

Antimony Tartrate Transition-Metal–Oxo Chiral Clusters

Qiang Gao, Xiqu Wang, Joshua Tapp, Angela Moeller, and Allan J. Jacobson*

Three homochiral heterometallic clusters composed of antimony tartrate transition-metal–oxo sandwiches have been obtained using a water-soluble chiral dimer $Sb_2(l\text{-tartrate})_2^{2-}$ as the precursor. These clusters consist of two different types of scaffolds that support different numbers and types of transition-metal cations. The flexibility of these chiral scaffolds is attributed to the versatile coordination modes of the l-tartrate ligand.

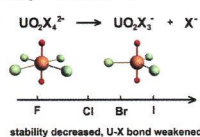


6617  dx.doi.org/10.1021/ic4006482

Probing the Electronic Structure and Chemical Bonding in Tricoordinate Uranyl Complexes $UO_2X_3^-$ ($X = F, Cl, Br, I$): Competition between Coulomb Repulsion and U–X Bonding

Jing Su, Phuong Diem Dau, Yi-Heng Qiu, Hong-Tao Liu, Chao-Fei Xu, Dao-Ling Huang, Lai-Sheng Wang,* and Jun Li*

The bonding and stability of a series of gaseous tricoordinate uranyl complexes $UO_2X_3^-$ ($X = F, Cl, Br, I$) have been investigated using photoelectron spectroscopy and relativistic quantum chemistry. U–X bonds in $UO_2X_3^-$ and $UO_2X_4^{2-}$ are dominated by ionic interaction with the bond strength, decreasing from F to I. All gaseous $UO_2X_4^{2-}$ dianions are metastable.

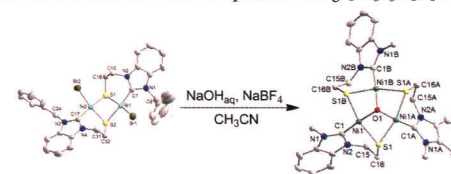



6627  dx.doi.org/10.1021/ic400672z

A Comparative Study on Dinuclear and Multinuclear Ni(II), Pd(II), and Pt(II) Complexes of a Thiolato-Functionalized, Benzannulated *N*-Heterocyclic Carbene Ligand

Dan Yuan and Han Vinh Huynh*

Dinuclear thiolato-bridged Ni(II) and Pt(II) NHC complexes **2** and **4** have been synthesized through a combined and in situ deprotonation/hydrolysis protocol of a thioester-functionalized benzimidazolium salt. Reactivity studies of **2** and **4**, and their previously reported Pd(II) analogue **1a** toward either Me_3OBF_4 , NaOH, or $Na_2S \cdot 9H_2O$ revealed clear differences, and led to the isolation of a series of trinuclear/tetranuclear NHC complexes bearing $[Ni_3S_3O]$, $[Pd_3S_3S]$, or $[Pt_4S_4]$ cores.

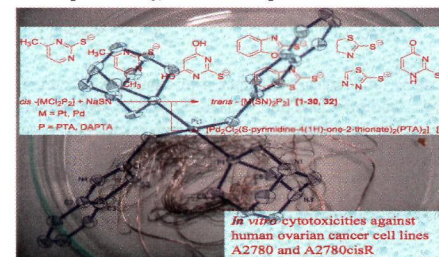


6635  dx.doi.org/10.1021/ic4006746

***trans*-Thionate Derivatives of Pt(II) and Pd(II) with Water-Soluble Phosphane PTA and DAPTA Ligands: Antiproliferative Activity against Human Ovarian Cancer Cell Lines**

Elena Guerrero, Susana Miranda, Sebastian Lüttenberg, Nils Fröhlich, Jan-Moritz Koenen, Fabian Mohr, Elena Cerrada, Mariano Laguna,* and Aránzazu Mendía*

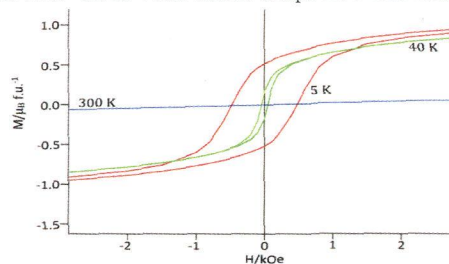
Palladium and platinum complexes of the type *trans*- $[M(SN)_2P_2]$, where P are the water-soluble phosphines PTA or DAPTA and HSN are eight selected heterocyclic thiones, were prepared. The X ray structures of six of the compounds confirm the *trans* disposition and, only in the case of $[Pd_2Cl_2(S\text{-pyrimidine-}4(1H)\text{-one-}2\text{-thionate})_2(PTA)_2]$, a dinuclear structure was observed. *In vitro* cytotoxicities against human ovarian cancer cell lines A2780 and A2780cisR were evaluated showing a high inhibition of cellular growth with a comparable IC_{50} to that of cisplatin.



La₃Ni₂SbO₉: a Relaxor Ferromagnet

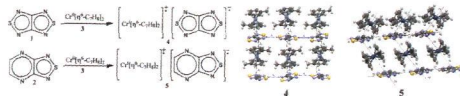
Peter D. Battle,* Sophie I. Evers, Emily C. Hunter, and Mark Westwood

Neutron diffraction and magnetometry have shown that Ni/Sb cation disorder causes the perovskite La₃Ni₂SbO₉ to behave as a relaxor ferromagnet below 105 K. The behavior stems from the need to distribute two cation species, present in a 2:1 ratio, over two crystallographically distinct six-coordinate sites that occur in a 1:1 ratio; one site is occupied exclusively by Ni²⁺, the other by a disordered arrangement of Ni²⁺ and Sb⁵⁺. This disorder disrupts the establishment of long-range magnetic ordering.

**Bis(toluene)chromium(I) [1,2,5]Thiadiazolo[3,4-c][1,2,5]thiadiazolidyl and [1,2,5]Thiadiazolo[3,4-b]pyrazinidyl: New Heterospin ($S_1 = S_2 = 1/2$) Radical-Ion Salts**

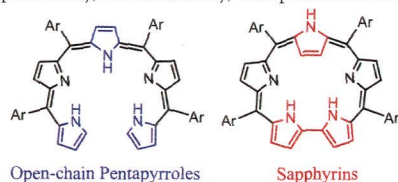
Nikolay A. Semenov, Nikolay A. Pushkarevsky, Elizaveta A. Suturina, Elena A. Chulanova, Natalia V. Kuratieva, Artem S. Bogomyakov, Irina G. Irtegov, Nadezhda V. Vasilieva, Lidia S. Konstantinova, Nina P. Gritsan,* Oleg A. Rakitin, Victor I. Ovcharenko, Sergey N. Konchenko, and Andrey V. Zibarev*

Bis(toluene)chromium(I) [1,2,5]thiadiazolo[3,4-c][1,2,5]thiadiazolidyl and [1,2,5]thiadiazolo[3,4-b]pyrazinidyl, the first representatives of a new class of heterospin ($S_1 = S_2 = 1/2$) radical-ion salts, were synthesized. The salts were characterized by X-ray diffraction and solid-state and solution electron paramagnetic resonance together with magnetic susceptibility measurements in the range 2–300 K. In the salts' spin systems, the dominance of antiferromagnetic exchange interactions was observed in agreement with the quantum-chemical calculations combined with simulation of the experimental $\chi T(T)$ dependences using the Van Vleck formula.

**Synthesis, Characterization, Protonation Reactions, and Electrochemistry of Substituted Open-Chain Pentapyrroles and Sapphyrins in Nonaqueous Media**

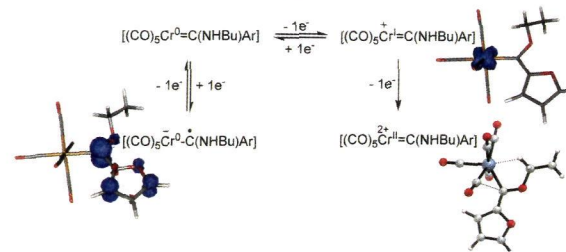
Mingzhu Yuan, Zhongping Ou,* Yuanyuan Fang, Shi Huang, Zhaoli Xue, Guifen Lu, and Karl M. Kadish*

Three open-chain pentapyrroles were isolated as side-products from the synthesis of triarylcorroles and then converted to the corresponding sapphyrins by catalytic oxidation in acidic media. The investigated compounds were characterized by UV–vis and ¹H NMR spectroscopy, mass spectrometry, electrochemistry, and spectroelectrochemistry.

**Substituent Effects on the Electrochemical, Spectroscopic, and Structural Properties of Fischer Mono- and Biscarbene Complexes of Chromium(0)**

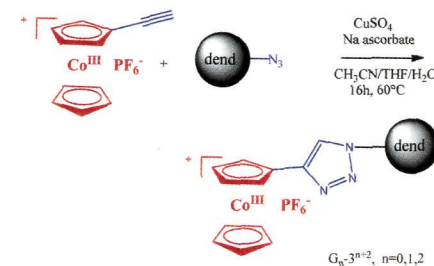
Belinda van der Westhuizen, Pieter J. Swarts, Louise M. van Jaarsveld, David C. Liles, Uwe Siebert, Jannie C. Swarts, Israel Fernández,* and Daniela I. Bezuidenhout*


The effect of both (hetero)aryl- and heteroatom-carbene substituent of a series of mono- and biscarbene complexes of Cr(0) were investigated by electrochemical, spectroscopic, and computational methods. Reversible Cr(0) oxidation was followed by an irreversible Cr(I) oxidation to form a dicationic Cr(II) species, characterized by unusual CH...Cr agostic interactions.

**'Click' Synthesis and Redox Properties of Triazolyl Cobalticinium Dendrimers**

Amalia Rapakousiou, Yanlan Wang, Colette Belin, Noël Pinaud, Jaime Ruiz, and Didier Astruc*

The derivatization of macromolecules with redox-stable groups is a challenge for molecular electronics applications. The large majority of redox-derivatized macromolecules involve ferrocenes, and there are only a few reports with cobalticinium. We report here the first click derivatization of macromolecules with the cobalticinium redox group using ethynylcobalticinium hexafluorophosphate, 1.

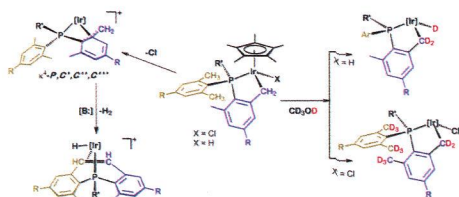


6694  dx.doi.org/10.1021/ic400759r

Cyclometalated Iridium Complexes of Bis(Aryl) Phosphine Ligands: Catalytic C–H/C–D Exchanges and C–C Coupling Reactions

Jesús Campos, María F. Espada, Joaquín López-Serrano, and Ernesto Carmona*

Complexes of the $[(\eta^5\text{-C}_5\text{Me}_5)\text{Ir}]$ unit with cyclometalated aryl phosphines can undergo exchange of the metalated and non-metalated aryl units. In addition to the uncommon $\kappa^4\text{-P,C,C',C''}$ binding mode that the metalated phosphine arm can adopt, this aryl interchange process accounts for the dehydrogenative C–C coupling and C–H/C–D exchange reactions of these species.

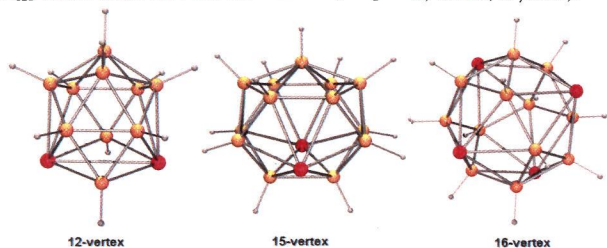



6705  dx.doi.org/10.1021/ic400761z

Supraicosahedral Polyhedra in Metallaboranes: Synthesis and Structural Characterization of 12-, 15-, and 16-Vertex Rhodaboranes

Dipak Kumar Roy, Bijan Mondal, Pritam Shankhari, R. S. Anju, K. Geetharani, Shaikh M. Mobin, and Sundargopal Ghosh*

The first example of a 15-vertex supraicosahedral metallaborane has been synthesized that exhibits hexacosahedron geometry. In parallel to the formation of 15-vertex cluster, a 16-vertex *isocloso*- $[(\text{Cp}^*\text{Rh})_3\text{B}_{12}\text{H}_{12}\text{Rh}\{\text{Cp}^*\text{RhB}_4\text{H}_8\}]$ and 12-vertex *isocloso*- $[(\text{Cp}^*\text{Rh})_2\text{B}_{10}\text{H}_{12}]$ rhodaboranes have also been isolated (see picture; Rh red, B yellow).

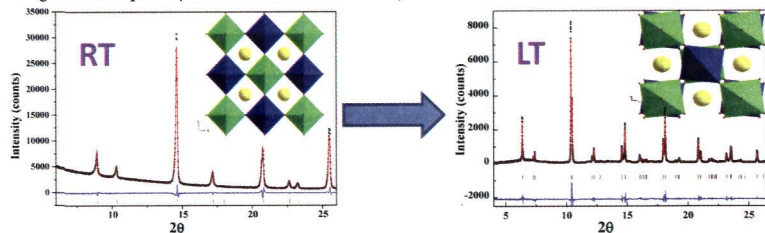


6713  dx.doi.org/10.1021/ic400740f

Synthesis, Crystal Structure, and Physical Properties of $\text{Sr}_2\text{FeOsO}_6$

Avijit Kumar Paul, Martin Jansen,* Binghai Yan, Claudia Felser, Manfred Reehuis, and Paula M. Abdala

The semiconducting double perovskite $\text{Sr}_2\text{FeOsO}_6$, which is pseudo-cubic at ambient conditions and tetragonal with space group $I4/m$ at lower temperature, displays two types of antiferromagnetic ordering of temperatures of $T_{\text{N}1} = 140$ K and $T_{\text{N}2} = 67$ K, respectively. The evolution of the magnetic ordering and nuclear structure with temperature has been monitored by heat capacity and magnetic susceptibility measurements as well as by PXRD.

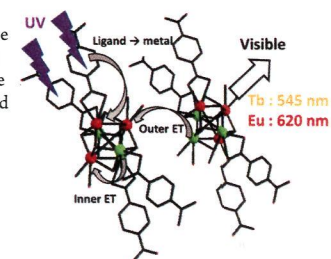


6720  dx.doi.org/10.1021/ic4008697

Coordination Polymers Based on Heterohexanuclear Rare Earth Complexes: Toward Independent Luminescence Brightness and Color Tuning

François Le Natur, Guillaume Calvez,* Carole Daguebonne, Olivier Guillou,* Kevin Bernot, James Ledoux, Laurent Le Pollès, and Claire Roiland

A family of monodimensional coordination polymers in which hexanuclear complexes act as metallic nodes has been synthesized. The hexanuclear cores can be either homometallic or heterometallic. Whatever the hexanuclear entities are, the resulting coordination polymers are iso-structural. The random distribution of the lanthanide ions over the six metallic sites of the hexanuclear entities is demonstrated by ^{89}Y -RMN, XRD, and luminescent measurements. In these compounds the independent tuning of luminescence intensity and color is possible.

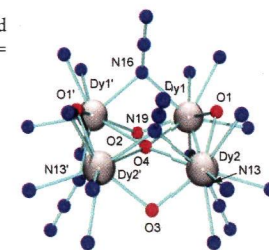



6731  dx.doi.org/10.1021/ic4008813

Self-Assembled $\text{Ln}(\text{III})_4$ ($\text{Ln} = \text{Eu}, \text{Gd}, \text{Dy}, \text{Ho}, \text{Yb}$) $[2 \times 2]$ Square Grids: a New Class of Lanthanide Cluster

Nicholas M. Randell, Muhammad U. Anwar, Marcus W. Drover, Louise N. Dawe, and Laurence K. Thompson*

Self-assembled $[2 \times 2]$ square $\text{Ln}(\text{III})_4$ grid complexes form using simple ditopic, bis-hydrazone ligands, with SMM behavior in the case where the $\text{Dy}(\text{III})$ ions are connected internally through $\mu_2\text{-O}_{\text{hydrazone}}$, $\mu_2\text{-oxide}$, and $\mu_2\text{-1,1-azide}$ bridges ($\tau_0 = 4.5 \times 10^{-7}$ s, $U_{\text{eff}} = 91$ K).

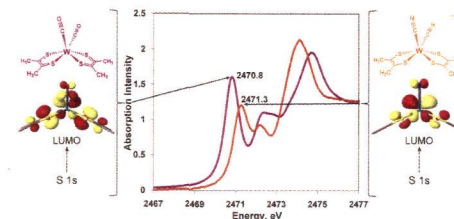


6743  dx.doi.org/10.1021/ic4009174

Ancillary Ligand Effects upon Dithiolene Redox Noninnocence in Tungsten Bis(dithiolene) Complexes

Yong Yan, Christopher Keating, Perumalreddy Chandrasekaran, Upul Jayarathne, Joel T. Mague, Serena DeBeer, Kyle M. Lancaster, Stephen Sproules, Igor V. Rubtsov, and James P. Donahue*

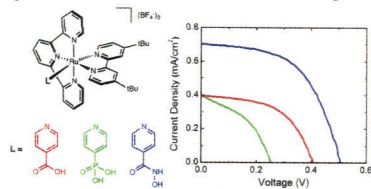
An expanded set of compounds of the type $[\text{W}(\text{S}_2\text{C}_2\text{Me}_2)_2\text{L}_1\text{L}_2]^n$ ($n = 0$: $\text{L}_1 = \text{L}_2 = \text{CO}$, **1**; $\text{L}_1 = \text{L}_2 = \text{CN}^t\text{Bu}$, **2**; $\text{L}_1 = \text{CO}$, $\text{L}_2 = \text{carbene}$, **3**; $\text{L}_1 = \text{CO}$, $\text{L}_2 = \text{phosphine}$, **4**; $\text{L}_1 = \text{L}_2 = \text{phosphine}$, **5, $n = 2^-$: $\text{L}_1 = \text{L}_2 = \text{CN}^-$, $[\text{6}]^{2-}$) has been synthesized and characterized. Despite isoelectronic formulations, the compound set reveals gradations in dithiolene ligand redox level as revealed by intraligand bond lengths, $\nu_{\text{C-C}_{\text{chelate}}}$ and rising edge energies in the sulfur K-edge X-ray absorption spectra (XAS). Differences between the terminal series members, **1** and $[\text{6}]^{2-}$, are comparable to differences seen in homoleptic dithiolene complexes related by full electron transfer to/from a dithiolene-based MO.**



Hydroxamate Anchors for Improved Photoconversion in Dye-Sensitized Solar Cells

Timothy P. Brewster, Steven J. Konezny,* Stafford W. Sheehan, Lauren A. Martini, Charles A. Schmuttenmaer,* Victor S. Batista,* and Robert H. Crabtree*

Water stable hydroxamate anchors are shown to give the highest overall sunlight-to-electricity conversion efficiency (η) in a systematic study of dye-sensitized solar cells fabricated using a novel series of ruthenium-polypyridyl sensitizers varying only in their anchoring group to TiO_2 . The obtained current density–voltage (J - V) characteristic curves have been modeled using the equivalent circuit model providing insight into the structure/function relationships that impact solar cell performance.

**Additions and Corrections****Correction to Serendipitous Assemblies of Two Large Phosphonate Cages: A Co_{15} Distorted Molecular Cube and a Co_{12} Butterfly Type Core Structure**

Javeed Ahmad Sheikh, Soumyabrata Goswami, Amit Adhikary, and Sanjit Konar*